https://doi.org/10.1016/j.trc.2019.11.004

Route and speed optimization for liner ships under emission control policies

Lu Zhen[a], Zhuang Hu[a], Ran Yan[b], Dan Zhuge[b,*], Shuaian Wang[b]

[a]School of Management, Shanghai University, Shang Da Road 99, Shanghai 200444, China
[b]Department of Logistics and Maritime Studies, The Hong Kong Polytechnic University, Hung Hom, Hong Kong

Abstract

Pollutants such as nitrogen oxides (NO_x), sulfur dioxide (SO_2), and particulate matters (PM) generated by shipping industry are increasing in recent years. In order to control the ship emission pollution, the International Maritime Organization (IMO) has established the Emission Control Areas (ECAs). In the fierce competition of the shipping market, liner shipping companies are looking for strategies to maintain their core competencies under the emission control policy. To achieve this goal, this paper first proposes a bi-objective mixed integer linear programming model, aiming to optimize sailing routes and speeds within and outside the ECA while minimizing the total fuel cost and SO_2 emissions. Then, a new algorithm is developed to solve the proposed model by combining the two-stage iterative algorithm and fuzzy logic method based on ϵ-constraint. Finally, this paper compares and analyzes the navigation plan of a real sailing route considering and not considering the effects of ECA. Some experiments are conducted to analyze the effects of fuel cost, decision makers, and ECA boundaries on the total fuel cost and SO_2 emissions. The results indicate that the proposed model and algorithm can contribute to save fuel cost and reduce SO_2 emissions under the ECA policy and provide different Pareto optimal solutions. Thus, the effectiveness of the model and the efficiency of the algorithm are validated.

Keywords: Emission Control Area (ECA), Bi-objective programming, Two-stage iterative algorithm, Route optimization, Sailing speed optimization.

*Corresponding author. dan.zhuge@connect.polyu.hk (Dan Zhuge).

1. Introduction

Shipping industry is an integral part of the global supply chain for global trade. Nearly 80% of the trade is carried out by sea, among which liner shipping transportation plays an important role. Recently, the impact of emission pollution on the environment caused by this low-cost transportation has received widespread attention. Research shows that emissions from the shipping industry are closely related to the fuel consumption, and the total fuel consumption is estimated to be between 279 million and 400 million tons per year (Cullinane and Bergqvist, 2014). Container liners emit large amounts of sulfur dioxide (SO_2), nitrogen oxides (NO_x), carbon dioxide (CO_2), and particulate matters (PM) in shipping process which seriously violate the concept of "green shipping".

Protecting the ecological environment is the prerequisite for long-term and sustainable use of resources. In order to reduce the serious environmental pollution brought about by the emissions of SO_2, NO_x, PM, and other pollutants, the International Maritime Organization (IMO) introduced the concept of Emission Control Area (ECA) in Annex VI of the International Convention for the Prevention of Pollution from Ships (MARPOL). The ECA includes the Baltic Sea area, the North Sea area, the North America area, and the United States Caribbean Sea area. Only fuel with no more than 0.1% of sulfur content can be used by ships within the ECAs since January 1, 2015 according to the regulations of IMO. Meanwhile, outside the ECA, only fuel with no more than 3.5% of sulfur content can be used.

In order to improve China's maritime environment, according to the national regulations and the international conventions, China has also promulgated related rules in 2015 and established the Domestic Emission Control Area (DECA) in three port areas, including Pearl River Delta, Yangtze River Delta and Bohai Rim (Beijing, Tianjin, Hebei). In December 2018, China further developed the related regulations to extend the ECA along the shoreline which has been implemented since January 1, 2019, as illustrated in Fig. 1. Since then, the ships within the DECA are required to use marine fuel with sulfur content no more than 0.5%.

Three emission reduction methods are widely used to meet the ECA sulfur standards (Fagerholt et al., 2015). (1) The first method is to use liquefied natural gas (LNG). LNG is one type of clean fuels with low sulfur contained and can fundamentally reduce SO_2 emissions. The drawback is the

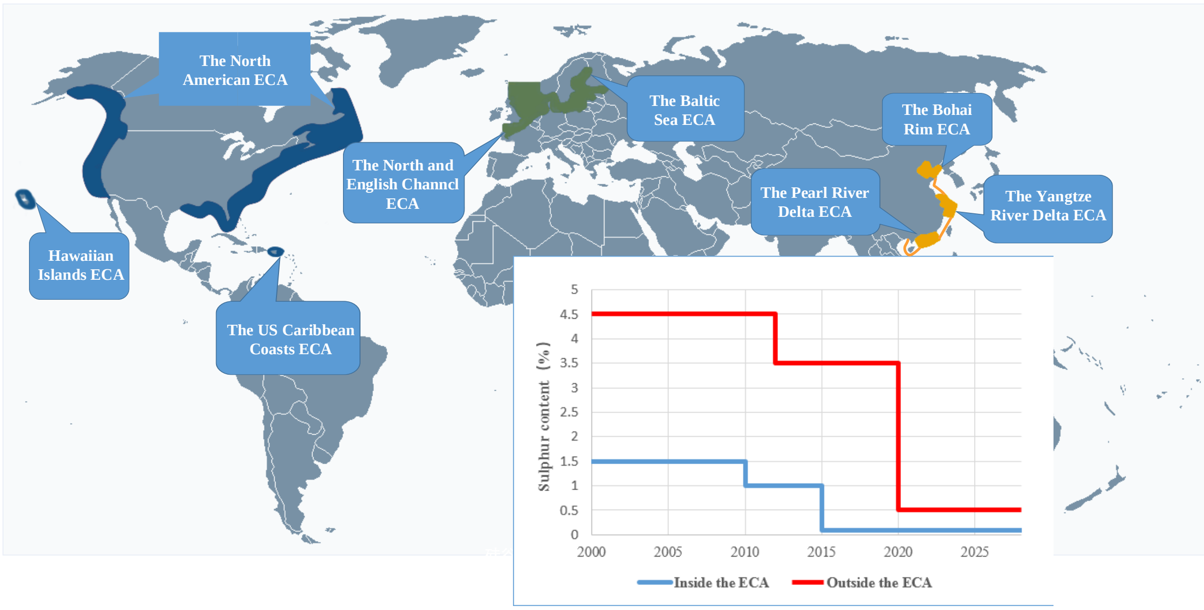

Figure 1: Emission Control Areas and the emission limits

high ship investment for storing and combusting the LNG on ships. In addition, it needs to be guaranteed that there are enough LNG supply facilities to provide the fuel for ships. (2) Installing the exhaust emission scrubber devices to filter the sulfur content in the exhaust gas is also an effective method. This method is mainly adopted by short-range offshore operators. For example, a shipping company called DFDS Seaways has begun a large-scale scrubber device installation plan, among which the costs for 21 ships reach 125 million dollars. As a result, the high cost for installing scrubber devices seriously confines their usage. (3) The third method is fuel switching, i.e., using fuel with a lower percentage of sulfur (e.g., marine gas oil (MGO)) within the ECA while using heavy fuel oil (HFO) outside the ECA, which is the most easily operated and widely used method under the condition of “green shipping”. In this paper, we will focus on the route and speed optimization to minimize the total fuel cost and SO_2 emissions when adopting the fuel switching method. Referring to some existing literature (Browning et al., 2012; Fagerholt et al., 2015; Gu and Wallace, 2017; Zhen et al., 2018), we assume that switching fuel is an instantaneous process in our paper for simplification.

The remainder of the paper is organized as follows. In section 2, we review the related literature. In section 3, we describe the problem and data used in this paper. In section 4, we introduce the mathematical model and the algorithm. Section 5 provides the results of the numerical experiment and discusses the experiment results. Concluding remarks are presented in the last section.

2. Literature review

With the fast development of the maritime industry, liner shipping has been widely studied and discussed. Meng and Wang (2012) put forward problems about liner ship planning under uncertain container transportation demand. Song and Dong (2012, 2013) studied issues related to container liner transportation. Bell et al. (2013) proposed a cost-based container allocation model for sea freight to minimize the total operating costs. Based on this study, Ng (2014, 2015) further studied the problems of the deployment of liner transport in a stochastic environment. Wang et al. (2015) analyzed the management of seasonal transportation revenue of the container companies. Song et al. (2015) constructed a cost optimization model to determine the number of ships, the maximum planned speed of navigation and the liner service schedule. Ng (2018) proposed a new approach to make a trade-off between ship sailing speed and the number of vessels required to maintain a given service frequency. Kisialiou et al. (2018, 2019) designed metaheuristic algorithms to analyze a tactical supply vessel planning problem. For the recent review on ship sailing speed optimization, readers are referred to Meng et al. (2014) and Wang and Meng (2017). As mentioned above, several practical optimization tools have been proposed.

There is also extensive literature focusing on reducing the emissions of SO_2 to improve the maritime environment by considering the three emission reduction methods mentioned above, i.e., using liquefied natural gas, installing the exhaust emission scrubber devices, and switching fuel by using MGO. Acciaro (2014) indicated that there was a balance between low fuel prices and LNG investment spending, and the development of LNG mainly depended on its future price, LNG ships capital cost and LNG engine's retrofitting cost. Jiang et al. (2014) made comparisons between scrubber devices installation and fuel switching and concluded that the final choice of the two approaches depended on the price gap between MGO and HFO. Boscaratoa et al. (2015) claimed that the development of a scrubber system for sea transport was still not mature enough as it was unable to process all pollutants produced by marine engines. Meanwhile, Hilmola (2015) reported that scrubber systems had not been widely used yet. The shipping companies were unable to complete the research for scrubbers and put them into use due to the insufficient time. The above two papers discussed some typical problems about the applications of the scrubber system in maritime transportation. Panasiu and Turkina (2015) analyzed the investment efficiency of scrubber device installation and calculated and evaluated the cost throughout the life cycle of the scrubber devices. Comparisons with the fuel switching method were made. Patricksson et al. (2015) formulated a stochastic model by using ECA as a key factor in the decision-making process. Minimization of the total expected cost was achieved by choosing from installation scrubber devices and fuel switching. Msakni and Haouari (2018) proposed a mixed integer programming model for an LNG short-term delivery planning problem that included several variables and constraints, such as time window, berth availability, bunker restriction, and inventory, with the objective to maximize the net profit.

Many scholars have studied the optimization of ship navigation scheme based on the concept of ECA or "green shipping". There are two main research areas. The first research area is to minimize total cost. Norstad et al. (2011) discussed a problem of tramp ship routing and scheduling while optimizing its sailing speed. In addition, a multi-start local search heuristic was proposed to solve the problem. Schinas and Stefanakos (2012) proposed a stochastic linear optimization model by minimizing the cost to determine the optimal ship matching scheme of the fleet under the restriction of ECA when the demand was uncertain. Experiment results indicated that some ships needed to re-arrange the routes if ECA was established. Lindstad et al. (2013) used fuel cost minimization as the objective function to evaluate the effects of ECA on emission reduction. The results showed that the best effect of reducing emissions depends on factors such as the power of the ship's engine, annual fuel consumption within ECA, and future fuel prices. Doudnikoff and Lacoste (2014) proposed a cost minimization model to estimate the combination of speed and the pollutant emissions from liner services when minimizing the internal and external costs. Fagerholt and Psaraftis (2015) and Fagerholt et al. (2015) proposed optimization models to minimize the operating costs of ships that travel along a particular sequence of ports. Zhen et al. (2018) put forward a mixed integer programming optimization model and minimized the total cost under the condition of ECA based on Tabu search algorithm. Wang et al. (2018) developed a mixed integer programming model which jointly designed the optimal ship sailing speed and the optimal amount of bunker fuel to purchase at each port in a shipping network in order to minimize the sum of ship operating costs and fuel costs. Psaraftis (2019) analyzed the combination problem of ship sailing speed and route optimization under the ECA policy. The regulatory dimension of speed reduction via speed limits was also discussed. Sheng et al. (2019) developed a mixed-integer convex minimization model to determine the optimal vessel speed and ship fleet size for an industrial shipping service operating within the ECAs. Minimizing SO_2 emissions is the second main research area. Kontovas (2014) proposed a general model for green ship routes and scheduling problems. Several alternatives are also offered to model ship emissions. Dulebenets et al. (2015) came up with an innovative mixed integer nonlinear programming model for green ship scheduling problems while taking the emission controls into consideration. Svindland (2018) introduced a method to calculate the SO_2 emissions in container liner and made a comparative analysis of SO_2 emissions before and after the implementation of ECA policy. The results showed that the emissions of SO_2 were reduced after the policy was implemented. Chen et al. (2018) constructed models on routes in container shipping to analyze the effect of ECA on the global shipping industry. It was identified that the emissions in the ECA would be highly reduced, while some ships had to re-plan the routes due to the implementation of ECA. Regarding single-objective optimization problems, some heuristic algorithms are proposed, such as x and y-clusters algorithm (Kim and Moon, 2003), dynamic programming technique (Park, 2003), time-space sequence pair (Moorthy and Teo, 2006) and construction heuristic based on priority list (Meisel and Bierwirth, 2009). Our model differs from the above studies in that we develop a bi-objective model that consider both costs and SO_2 emissions.

Bi-level models are generally difficult to solve and a number of scholars are interested in developing algorithms to solve them. Some algorithms, such as evolutionary algorithm and ant colony algorithm, are adopted to address bi-objective planning problems (Cheong and Tan, 2008). However, the algorithms can only be applied to solve the discrete problems instead of continuous problems. To address the continuous multi-objective problems, the existing literature focuses on preference-based method and generating method (Yeung and Man, 2011; Demir et al., 2014). The former method considers the preferences of the decision makers through goal programming and global criterion methods but can only provide a single solution. There are many ways to generate solutions by using the latter method, such as weighted sum, evolutionary method, and ϵ-constraint method, to generate a set of Pareto optimal solutions. The advantage of the latter method is that it can provide a set of solutions for the decision makers to choose from (Tian et al., 2016a, 2016b). In the above mentioned methods, different weight combinations in the weighted sum may lead to the same solution, and the objective function must be transformed to the same scale before a weighted sum is formed. In addition, it is difficult to control the number of Pareto solutions. Although evolutionary methods can provide a set of approximate Pareto solutions, these solutions could be far away from the optimal Pareto solutions. The ϵ-constraint method (Bérubé et al., 2009) is the most effective method especially for bi-objective optimization problems. It can convert the original bi-objective problem into a set of single-objective problems and take less time to obtain the required number of Pareto solutions (Mavrotas, 2009; Li et al., 2016). Therefore, the paper proposes a two-stage iterative method based on ϵ-constraint method. This method covers a larger search space so that it can find a more reasonable trade-off solution for the bi-objective optimization problem.

To sum up, most of the literature focuses on establishing a single objective function to optimize the shipping process. There is a lack of research on the construction of bi-objective models and algorithms for speed and route optimization problems. With the development of "green shipping", the ECA policy will undoubtedly influence the choices of container transport navigation programs. This paper constructs a bi-objective optimization model to minimize the total fuel cost and total SO_2 emissions as well as analyzes the effectiveness of the proposed algorithm by using historical operating data from a liner shipping company. The CPLEX solver is used to solve the model. We also conduct some experiments to examine the effects of fuel cost, decision makers, and ECA boundaries on the total cost and SO_2 emissions.

3. Problem description and basic data

3.1. Problem description

The global maritime environment has been improved after the ECA is introduced by the IMO, but it also brings some new problems to the shipping industry. For example, how to design the navigation plans under the ECA policy and how to minimize shipping emissions are important issues that need to be considered by the shipping industry. In order to address the above problems, this paper proposes a bi-objective optimization mathematical model for container liner ship route design and speed optimization under the ECA policy. Considering several port cities and the arrival time, we minimize the total fuel cost and total SO_2 emissions by optimizing the sailing route and the speed within and outside the ECA.

The first objective of the model is to minimize the total cost. There are many costs involved in the container shipping process. Based on related literature, route and speed selection will have little impact on some nearly fixed costs, including labor cost, repair cost, and inventory cost. Therefore, this paper only considers the fuel cost as it will be affected by the change of route and speed and it constitutes a large percentage of the total operating cost.

Apart from that, the main pollutants emitted by container liners during navigation are SO_2, CO_2 and NO_x. SO_2 emissions from ocean-going ships are proportional to the sulfur content of the total fuel used, fuel consumption, and a proportional constant called the "sulfur index", which can be calculated as multiplying the total fuel consumption (tons) by the percentage of sulfur in the fuel (e.g., 4%, 1.5%, 0.5%), and then multiplied by 0.02 (Dulebenets, 2017; Bergqvist et al., 2015). The whole process can be explained by the chemical reaction of sulfur and oxygen, in which only 2% of the sulfur can react with oxygen to generate SO_2. For example, 100 tons of fuel containing 3.5% sulfur can emit 7 tons of SO_2, and the same amount of fuel with a sulfur content of 0.1% produces only 0.2 tons. Thus, reducing SO_2 emissions can be achieved by burning less high sulfur fuel or using cleaner fuel with lower sulfur content. The calculation formula of the amount of SO_2 emissions is as follows:

The amount of SO_2 emissions $= 0.02 \times$ total fuel consumption $\times$ percentage of sulfur in fuel.

According to the regulations of IMO, since 2012, ships all over the world are required to use fuel with a sulfur percentage at most 3.5 (e.g., HFO) (Kontovas, 2014). After introducing the ECA in 2015, ocean ships need to use MGO instead of HFO during their voyage in ECAs such as the Baltic Sea area, the North Sea area, the North America area and the United States Caribbean Sea area. Since January 1, 2019, sea-going ships entering the DECA in China need to use marine fuel with a sulfur content no more than 0.5% (e.g., MGO) and may follow the international standard of 0.1% in the future. Thus, MGO with no more than 0.1% sulfur and HFO with 3.5% sulfur are studied in our experiments.

Ships will also emit considerable CO_2 and NO_x. The amount of CO_2 emissions is proportional to the amount of fuel used, and the proportionality constant is often called the "carbon factor". The factor was 3.17 (tonnes of CO_2 per ton of fuel) in the first IMO greenhouse gas study published in 2000. However, the factor value was updated to a lower value in the second IMO greenhouse gas study in 2009, ranging from 3.021 of HFO to 3.082 of MGO (Psaraftis and Kontovas, 2013).

The carbon factor of natural fuels such as LNG can be between 2.6 and 2.8. CO_2 emissions can be calculated based on the total fuel consumption and CO_2 emission factor of the voyage, i.e.,

The amount of CO_2 emissions = Total fuel consumption × Carbon dioxide emission factor.

Similarly, the amount of NO_x can be calculated by using the total fuel consumption and NO_x emission factor, where the NO_x emission factor is between 0.057 and 0.087 (Dulebenets, 2017), i.e.,

The amount of NO_x emissions = Total fuel consumption × Nitrogen oxides emission factor.

We focus on SO_2 emissions in this paper. According to the research by Zhen et al. (2018), the total amount of SO_2 emitted by ocean-going vessels in the world is about 4.7-6.5 Tg per year, which accounts for more than 8% of anthropogenic emissions. SO_2 is a major pollutant emitted by ocean-going ships, which may produce acid rain and cause serious harm to human, animals and plants. At the same time, under the action of light and oxidant, SO_2 will react to form a sulfate gas solution, which will aggravate the deterioration of haze. Hence, the second objective of the model is to minimize the total SO_2 emissions.

3.2. Basic data

3.2.1. Fuel price

Fuel prices vary among different ports. Based on data from the website of "eworldship", the price of HFO fluctuates between 345 and 465 USD/ton from December 2017 to December 2018, while the price for MGO fluctuates between 500 and 1160 USD/ton. Taking the uncertainty of fuel prices into account, the prices of HFO and MGO are key factors for the speed and route decision-making in this paper. It is possible for a ship to refuel at any port during its voyage, and thus this paper adopts the average fuel price of different regions all over the world in our experiments, i.e., the price for MGO used within the ECA is set to be 750 USD/ton, and the price for HFO used outside the ECA is set to be 405 USD/ton.

3.2.2. Fuel consumption

The research conducted by Du et al. (2011), Wang and Meng (2012), and Psaraftis and Kontovas (2013, 2014) showed that the relationship between the sailing speed and bunker consumption is nonlinear, and the daily bunker consumption is approximately proportional to the sailing speed cubed. Thus, the fuel consumption per unit of distance is a function proportional to the sailing speed squared, i.e., a convex function of speed.

The shipping company will record the fuel consumption of each ship at some speeds during its actual voyage. As the speed and fuel consumption have an approximate non-decreasing convex function relationship, by combining with the piecewise linear interpolation method, the fuel consumption at any speed can be estimated. For example, suppose that two speed point a and b are recorded, a speed point c between a and b can be calculated by using the piecewise linear interpolation method. The computational results are slightly higher than the actual values. Since the speed point recorded by the shipping company is generally a series of integer value points in continuous time, the deviations of the corresponding fuel consumption of the non-integer velocity are quite small, and hence the errors can be ignored.

In our experiments, fuel consumption values (tons) corresponding to discrete speed values are given by Fig. 2 (i.e., the fuel consumptions of ships sailing per 500 nautical miles). The minimum and maximum sailing speeds are 15 knots and 21 knots, respectively. It can be seen from Fig. 2 that the fuel consumption gradually increases with the increase of speed and the upward trend continues to expand.

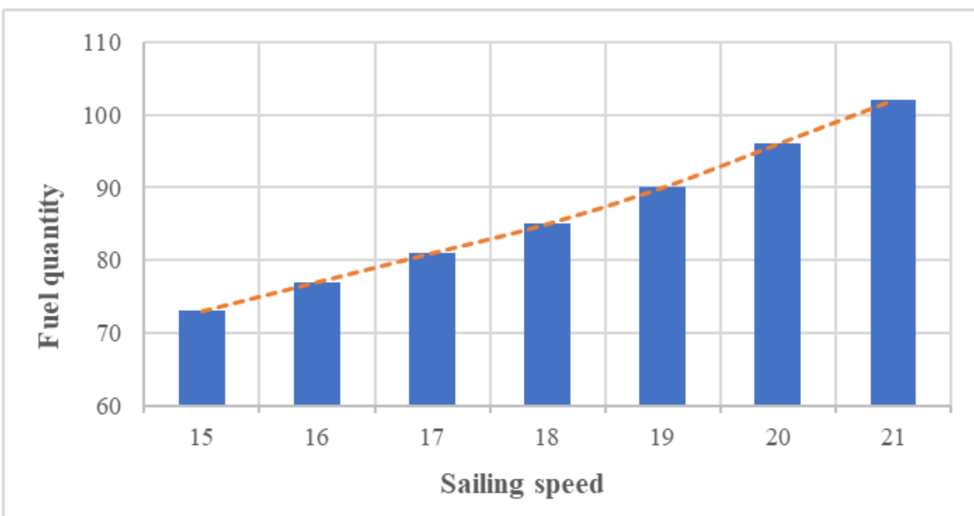

Figure 2: Fuel consumption of ships sailing 500 nautical miles (Zhen et al., 2018)

3.2.3. Time window

In this study, each port on a route is related to a time window so that ships will visit each port at the proper time. These time windows can be derived from contracts on the loading and unloading of goods with the customers and can also be a time period agreed between the shipping companies and the port operators. Taking the convenience of operation into consideration, all the arrival times are set at daytime. For example, in the case of Shanghai Zhonggu Shipping Group Co., Ltd, the ships depart from Dalian at 12 AM on day 0 and arrive at the second port (Yantai) during 8 AM and 4 PM on the x^{th} ($0 \leq x \leq 10$) day. The ships are supposed to stay at the port for 11 hours to load and unload cargoes before departing for the next port. The arrival time window and staying time at each port are the same. The latest time for the ship to return to the first port (Dalian) is 4 PM on the tenth day.

4. Mathematical model

Indices and Sets

i, j	Index of port .
k	Number of days of the voyage from port i to j.
v	Sailing speed of ships.
r	Index of path options of a ship, r=1,2,3$\cdots$.
A	Set of ports of call, A={0,1,$\cdots$,N,N+1}, in which 0 and N+1 are the home port.
G	Set of two consecutive ports of call, $G=\{ij \mid$a ship first visits port i then visits $j=i+1\}$, $i=0,\cdots,N$.
K	Set of voyage days from port i to port j.
V	Set of speeds at discrete points.
R_{ij}	Set of path options from port i to port j.
RE_{ij}	Set of path options containing stretches within the ECA from port i to port j, $RE_{ij} \in R_{ij}$.
RN_{ij}	Set of path options containing stretches outside the ECA from port i to port j, $RN_{ij} \in R_{ij}$.

Input parameters

P^{ECA}	Fuel price within the ECA.
P^{N}	Fuel price outside the ECA.
F_{ijrv}^{ECA}	Fuel consumption within the ECA for a sailing from port i to port j when choosing path option r and sailing at speed v .
F_{ijrv}^{N}	Fuel consumption outside the ECA for a sailing from port i to port j when choosing path option r and sailing at speed v .

T_{ijrv}^{ECA}	Sailing time within the ECA for a sailing from port i to port j when choosing path option r and sailing at speed v .
T_{ijrv}^{N}	Sailing time outside the ECA for a sailing from port i to port j when choosing path option r and sailing at speed v .
C_{ijrv}^{ECA}	Emissions of SO_2 within the ECA for a sailing from port i to port j when choosing path option r and sailing at speed v .
C_{ijrv}^{N}	Emissions of SO_2 outside the ECA for a sailing from port i to port j when choosing path option r and sailing at speed v .
γ_i	Waiting time of ships at port i.
L_{jk}	Lower bound of time window when the ships arrive at port j on day k.
E_{jk}	Upper bound of time window when the ships arrive at port j on day k.
M	A sufficiently large positive number.

Decision variables

t_j	Time when the ship arrives at port j.
s_{ij}	Sailing time of a ship between port i and port j.
y_{ijrv}^{ECA}	Weight of sailing speed v within the ECA for a sailing from port i to port j under the path option r .
y_{ijrv}^{N}	Weight of sailing speed v outside the ECA for a sailing from port i to port j under the path option r .
z_{ijr}	Binary variable, equal to one if path option r is chosen when the ship sails from port i to port j, and zero otherwise.
β_{jk}	Binary variable, equal to one if the ship arrives at port j on day k, and zero otherwise.

Mathematical model

$$\min Z_1 = \sum_{i,j \in G} \left(\sum_{r \in RE_{ij}} \sum_{v \in V} P^{ECA} F_{ijrv}^{ECA} y_{ijrv}^{ECA} + \sum_{r \in RN_{ij}} \sum_{v \in V} P^{N} F_{ijrv}^{N} y_{ijrv}^{N} \right) \tag{1}$$

$$\min Z_2 = \sum_{i,j \in G} \left(\sum_{r \in RE_{ij}} \sum_{v \in V} C_{ijrv}^{ECA} y_{ijrv}^{ECA} + \sum_{r \in RN_{ij}} \sum_{v \in V} C_{ijrv}^{N} y_{ijrv}^{N} \right) \tag{2}$$

subject to:

$$s_{ij} = \sum_{r \in R_{ij}} \sum_{v \in V} \left(T_{ijrv}^{ECA} y_{ijrv}^{ECA} + T_{ijrv}^{N} y_{ijrv}^{N} \right) \quad \forall i, j \in G \tag{3}$$

$$t_i + \gamma_i + s_{ij} \leq t_j \quad \forall i, j \in G \tag{4}$$

$$t_j - M(1 - \beta_{jk}) \leq E_{jk} \quad \forall j \in A, k \in K \tag{5}$$

$$t_j + M(1 - \beta_{jk}) \geq L_{jk} \quad \forall j \in A, k \in K \tag{6}$$

$$\sum_{k \in K} \beta_{jk} = 1 \quad \forall j \in A \tag{7}$$

$$\sum_{v \in V} y_{ijrv}^{ECA} = z_{ijr} \quad \forall i, j \in G, r \in RE_{ij} \tag{8}$$

$$\sum_{v \in V} y_{ijrv}^{N} = z_{ijr} \quad \forall i, j \in G, r \in RN_{ij} \tag{9}$$

$$\sum_{r \in R_{ij}} z_{ijr} = 1 \quad \forall i, j \in G \tag{10}$$

$$y_{ijrv}^{ECA} \geq 0 \quad \forall i, j \in G, r \in RE_{ij}, v \in V \tag{11}$$

$$y_{ijrv}^{N} \geq 0 \quad \forall i, j \in G, r \in RN_{ij}, v \in V \tag{12}$$

$$t_i \geq 0 \quad \forall i \in A \tag{13}$$

$$\beta_{jk} \in \{0, 1\} \quad \forall j \in A, k \in K \tag{14}$$

$$z_{ijr} \in \{0, 1\} \quad \forall i, j \in G, r \in R_{ij} \tag{15}$$

The objective (1) aims to minimize the sum of the fuel cost within and outside the ECA. As the fuel consumption and speed have a nonlinear relationship, the piecewise linear interpolation method is adopted to estimate the fuel consumption at a certain speed based on the decision variables $y_{ijrv}^{ECA}$and y_{ijrv}^{N}. The target of objective (2) is to minimize the total SO_2 emissions within and outside the ECA. Constraints (3) and (4) guarantee that the allowable arrival time to a port plus the port time and sailing time to the next port will not exceed the allowable arrival time to the next port. Constraints (5-7) ensure that the allowable arrival time is within the time window. Constraints (8) and (9) connect the path option with voyage speed weight, i.e., if path option r is chosen, the sum of speed weight within and outside the ECA is equal to one, respectively. Constraint (10) ensures that one path option must be selected from port i to port j. Constraints (11-13) guarantee that the speed weight and arrival time are nonnegative. Constraint (14) and (15) ensure the domains of β_{jk} and z_{ijr}. As the proposed model is an NP-hard problem, this paper designs a two-stage iterative and fuzzy decision algorithm based on ϵ-constraint to solve the model.

Bi-objective decision making method for mathematical planning is a popular method used to address the bi-objective optimization problems. Generally, the bi-objective problem is turned to single-objective problems at first, and then multiple solutions are found for these single-objective problems in order to get the Pareto optimal solution set. One of the efficient methods to get the Pareto solution is the ϵ-constraint method (Haimes et al., 1971). It has other advantages including but not limited to working without other parameters and with a unified dimension. The bi-objective optimization problem in this paper is presented as follows,

$$\min \quad F_1 = \varphi(x) \tag{16}$$

$$\min \quad F_2 = \omega(x) \tag{17}$$

$$\text{s.t.} \quad x \in X, \tag{18}$$

where x is the decision vector for all decision variables, $\varphi(x)$ and $\omega(x)$ represent the total fuel cost and total SO_2 emissions, respectively, and X is the feasible region of x defined by constraints (3-15). If $\varphi(x) \leq \varphi(x')$, $\omega(x) \leq \omega(x')$, and at least one of the two objectives is strict inequality, a feasible solution $x \in X$ is strictly better than and hence can replace another feasible solution $x' \in X$. Meanwhile, if no feasible solution $x' \in X$ can replace the existing feasible solution $x^* \in X$, then the existing solution is irreplaceable, i.e., it is a Pareto optimal solution. The corresponding value of the objective $(\varphi(x^*), \omega(x^*))$ is the Pareto point, and the Pareto optimal solution set is defined as $P_s = \{x^* \in X | x^* \text{ is a Pareto optimal solution}\}$. The Pareto frontier is defined as $P_f = \{(\varphi(x^*), \text{Ø}(x^*)) | x^* \in P_s\}$.

The basic idea for the ϵ-constraint method is to transform the initial bi-objective programming problem (i.e., the problem defined by (16) to (18)) into a single-objective programming problem with a primary objective. In other words, we need to turn the initial objective (e.g., to minimize $\omega(x)$) into the constraint limited by parameter ϵ ($\omega(x) \leq \epsilon$) and solve the sequences (i.e., to minimize $\varphi(x)$). In this paper, the goal is to turn the bi-objective function into two single-objective optimization problems. The whole problem can be viewed as two sub-problems: problem A: setting the minimization of total fuel cost as the goal while the total SO_2 emissions as the constraint; problem B: setting the minimization of the total SO_2 emissions as the goal while the total fuel cost as the constraint. The definitions of the two problems are as follows.

$$\text{Problem A :} \qquad \min \{\varphi(x)|\omega(x) \leq \epsilon, x \in X\} \tag{19}$$

$$\text{Problem B :} \qquad \min \{\omega(x)|\varphi(x) \leq \epsilon, x \in X\} \tag{20}$$

The possible values of ϵ lie in an interval in this problem. In order to construct the Pareto optimal solution set, a two-stage iterative approach of the ϵ-constraint method can be adopted to obtain the ideal point (f_1^I, f_2^I) and farthest point(f_1^N, f_2^N) to determine the value range. The lower and upper bounds of the Pareto optimal solution value are defined by the ideal and farthest points respectively. They can be generated by solving the following single-objective problems.

$$f_1^I = \min \{\varphi(x)|x \in X\} \tag{21}$$

$$f_2^I = \min \{\omega(x)|x \in X\} \tag{22}$$

$$f_1^N = \min \{\varphi(x)|\omega(x) = f_2^I, x \in X\} \tag{23}$$

$$f_2^N = \min \{\omega(x)|\varphi(x) = f_1^I, x \in X\} \tag{24}$$

Firstly, the lower bounds of the two objective functions can be solved according to the two single-objective problems respectively. Then, the upper bound of the two objective functions can be figured out based on problems defined by (19) and (20). In this way, the approximate ideal point (f_1^I, f_2^I) and approximate farthest point (f_1^N, f_2^N) can be generated, and the value of ϵ can also be identified based on the range of $[f_2^I, f_2^N]$. By setting the step Δ to find out the value of ϵ, a series of single-objective optimization problems can be formed and the Pareto frontier or its approximation can be obtained after solving them. In other words, after fixing the value of ϵ, there is always a solution $x' = x(\epsilon)$ for each single-objective function. If there is no $x \in X$ that satisfies $f(x) < f(x')$, then x' is the optimal Pareto solution of the initial problem, and all Pareto optimal solutions form the surfaces of the Pareto frontier.

As several sub-problems of ϵ need to be addressed in the two-stage iterative approach, the Pareto solution set will contain several solutions. In order to obtain the optimal solution according to the demand of the decision makers, fuzzy decision method is used to get an optimal solution, as this method can generate the optimal degree of the selected solution according to the decision makers' preference. Linear membership functions of the Pareto objective functions are first generated by the following formulas:

$$\delta_i(f_i^s) = \begin{cases} 1 & f_i^s \leq f_i^I \\ \frac{f_i^N - f_i^s}{f_i^N - f_i^I} & f_i^I < f_i^s < f_i^N, i = 1, 2; 1 \leq s \leq S, \\ 0 & f_i^s \geq f_i^N \end{cases} \tag{25}$$

where $\delta_i(f_i^s)$ represents the i^{th} objective function of the s^{th} solution, and f_i^I and f_i^N are the lower bound and upper bound of the i^{th} objective function, while f_i^s is the s^{th} Pareto solution in the i^{th} objective function. The total membership degree δ^s is calculated by the following formula:

$$\delta^s = \sum_{i=1}^{2} \omega_i \delta_i(f_i^s), \tag{26}$$

where ω_i is the weight of the i^{th} objective, and in this model $\sum_{i=1}^{2} \omega_i = 1$. It can be determined by the preference of the decision makers and the optimal solution is the solution with the maximum δ^s.

It is worth mentioning that the selected method is better than the weighted sum. Although the two methods both need to consider the preference of the decision makers, the meanings of the weights are different. In the weighted sum, weights are attached directly to each objective. Nevertheless, it can be challenging as these objectives usually have different units and dimensions. In addition, if the decision makers change their minds, a new set of weights need to be estimated to reflect their preference and new problems need to be addressed. On the contrary, in the fuzzy decision method, the weights are attached to the membership degrees of each objective and all these membership degrees are standardized into scalar ranging from 0 to 1 which makes it possible to get the Pareto optimal solution set at the selecting stage. More importantly, when the decision makers change their mind, all that need to do is to estimate a new set of weights and choose a new solution in the Pareto optimal solution set.

5. Numerical examples

5.1. Example description

According to the IMO regulations of sulfur emission controls on ships, from January 1, 2015, ships should use fuel containing no more than 0.1% of sulfur in the ECA of the Baltic Sea area, the North Sea area, the North America area, and the United States Caribbean Sea area. Since January 1, 2020, sulfur contained in ship fuel should be no more than 0.5% worldwide. This means that it is necessary to take appropriate measures to reduce sulfur emissions from ships. At the same time, container liner routes in other regions of the world will also be affected by the European and North American ECA regulations.

Figure 3: Navigation plans of the example

Based on the newly introduced regulations from December 2018, China has expanded its ECA along the coastline. To better demonstrate the influence of ECA on liner shipping and validate the effectiveness of the proposed model, a shipping route in Shanghai Zhonggu Shipping Group Co., Ltd., is discussed as a case in this section. The container liners depart from Dalian which is located in the DECA, then call at Yantai, Shanghai, Ningbo, and Shenzhen, and finally return to Dalian. The locations of the ports are illustrated in Fig. 3, where the boundary of ECA is marked by a

Figure 4: Five path options from Ningbo to Shenzhen

blue dotted line, and the route is shown by a red line.

The route is generated by BLM-Shipping, which is based on several electronic maps. It can position and search the current and history ship tracks based on the AIS data. It can also be used to calculate the distances between two ports, design shipping routes, and monitor the voyages. Based on the coordinates of DECA given by the Ministry of Transport of the People¡s Republic of China, the boundaries of DECA can be illustrated in Fig. 3 and the shipping routes can be generated based on the designated points at sea. According to the ports on the shipping routes of Shanghai Zhonggu Shipping Group Co., Ltd., our study takes a route with five legs into consideration. The possible path options for a leg from Ningbo to Shenzhen are illustrated in Fig. 4 in red solid lines.

The sailing distances within and outside the ECA corresponding to the five legs are illustrated in Table 1.

Table 1: Sailing distances within and outside the ECA for five legs in each path option

Cities	Option 1	Option 2	Option 3	Option 4	Option 5
1 Dalian – 2 Yantai	183/0	164/21	144/42	123/63	102/84
2 Yantai – 3 Shanghai	113/216	184/315	153/346	125/375	96/403
3 Shanghai – 4 Ningbo	193/0	163/69	132/137	91/176	49/214
4 Ningbo – 5 Shenzhen	738/0	237/562	195/603	155/644	114/684
5 Shenzhen – 1 Dalian	359/1399	363/1468	366/1547	326/1673	285/1788

Note: For "183/0", "183" is the distance within the ECA and "0" is the distance outside the ECA.

5.2. Numerical experiments

To solve the model proposed in Section 4, in this section, numerical experiments are conducted on a PC (processor Intel Core i7, 2.50 GHz, 8GB RAM). The model is solved by using C# to call the interface of CPLEX 12.6 on VS2015.

5.2.1. Performance of the model considering the effects of ECA

A case study of a shipping route operated by Shanghai Zhonggu Shipping Group Co., Ltd. is conducted in our study. In this case, the ships depart from Dalian, then visit Yantai, Shanghai, Ningbo, and Shenzhen in sequence, and finally return to Dalian. The path and speed solution without considering the effects of ECA is obtained as follows. To begin with, we do not consider the ECA regulations. Option 1 which provides the shortest distance between any two ports is selected and the total distance of the route is 3,201 nautical miles. Based on Fig. 2 and the piecewise linear interpolation method introduced in Section 3.2.2, the fuel consumption can be calculated by the real sailing speed and the shortest sailing path. Then, different types of fuel used within and outside the ECA are taken into consideration to calculate the total fuel cost and SO_2 emissions, and the results are illustrated in Table 2. The total fuel cost is about 352,595.24 USD, and the total SO_2 emissions is 23.917 tons. The fuel consumption within the ECA is 290.098 tons while the amount outside the ECA is 333.387 tons, and the total fuel assumption is 623.485 tons.

When the weights of the membership degrees are the same for the two objectives, the results considering the effects of ECA are illustrated in Table 3. It can be seen that the fuel cost is about 258,899.15 USD. Compared with the fuel cost not considering the effects of ECA, about 93,696.09 USD (26.57%) can be saved. The total SO_2 emission is increased to 29.148 tons, with a rise of

Table 2: The results without considering the effects of ECA

Leg	Speed (knots)		Fuel consumption (tons)			Fuel cost (USD)	SO_2 emissions (tons)
	Within ECA	Outside ECA	Within ECA (MGO)	Outside ECA (HFO)	Total fuel consumption		
1-2	15.000	–	26.718	–	26.718		
2-3	20.560	20.560	22.455	82.924	105.379		
3-4	19.300	–	35.435	–	35.435	352595.24	23.917
4-5	19.946	–	141.218	–	141.218		
5-1	18.903	18.903	64.272	250.463	314.735		
Total	–	–	290.098	333.387	623.485		

Table 3: The results considering the effects of ECA

Leg	Option	Speed (knots)		Fuel consumption (tons)			Fuel cost	Cost saved	SO_2 emissions	Emission increased
		Within ECA	Outside ECA	Within ECA	Outside ECA	Total fuel consumption	(USD)	(USD)	(tons)	(tons)
1-2	5	15.000	15.471	14.892	12.581	27.473				
2-3	5	15.222	15.222	14.186	59.554	73.740				
3-4	2	15.000	16.000	23.798	10.626	34.424	258899.15	93696.09	29.148	5.231
4-5	5	15.322	19.338	16.938	125.894	142.832				
5-1	1	15.000	15.000	52.414	204.254	256.668				
Total	–	–	–	122.228	412.909	535.137				

5.231 tons. As shown in Table 3, the shipping fuel consumption within the ECA is 122.228 tons, while the consumption outside the ECA is 412.909 tons, and the total fuel consumption is 535.137 tons. The total distance of the route is 3,473 nautical miles. In this case, three legs choose option 5, meaning the container liners prefer the routes with longer total distance but shorter distance in the ECA to reduce the cost. However, the price of fuel within the ECA (MGO) is higher than the price of fuel outside the ECA (HFO), and the sailing speed outside the ECA is larger than or equal to the speed within the ECA. For instance, for the sailing leg from Dalian to Yantai, the ship sails at the lowest speed of 15 knots within the ECA to minimize the fuel consumption, while when sailing outside the ECA, the sailing speed needs to be increased to make up for the extra time spent within the ECA. The results of the optimization model validate the influence of ECA on shipping industry as presented in the introduction part.

5.2.2. Effect of fuel price

Different fuel prices within and outside the ECA will have a great impact on the navigation cost. In the baseline scenario, the price for MGO is 750 USD/ton. Assume that the price for HFO remains unchanged and we analyze the impact of fuel price on total costs by setting the price of MGO as 850, 950, 1,050 and 1,150 USD/ton respectively. By adopting the calculation process proposed in Section 5.2.1, the fuel cost considering and not considering the effects of ECA are presented in Table 4.

Table 4: Comparison of the fuel cost under different prices of MGO

MGO price	Fuel cost (USD)		Cost saved (USD)
(USD/ton)	Not considering the effects of ECA	Considering the effects of ECA	
750	352595.24	258899.15	93696.09
850	381605.04	271121.95	110483.09
950	410614.84	283344.75	127270.09
1050	439624.64	295567.55	144057.09
1150	468634.44	307790.35	160844.09

As illustrated in Table 4, the proposed model can reduce the fuel cost under each of the price condition significantly. From the perspective of cost saving, the higher the price of MGO, i.e., the larger difference of the fuel prices within and outside the ECA, the more costs can be saved when the effects of ECA are considered. When the price of MGO is 1,150 USD/ton, the cost saving reaches 160,844.09 USD, which is about 34.32% of the fuel cost when the effects of ECA are not considered. Therefore, the model can help the shipping companies to reduce the cost by optimizing the sailing speed and routes. It should be noted that the savings listed in the table are just for one voyage. For a ship company with more similar routes, more savings can be obtained by adopting the proposed model. If the companies take the impact brought by the ECA into account, each ship is expected to save hundreds of thousands of or even millions of dollars in fuel cost each year if the sailing speed and routes can be optimized after re-designing the voyage scheme. Also, the model can be applied to other routes.

5.2.3. *Effect of decision maker*

It is shown in Section 5.2.1 that the objectives of minimizing the total fuel cost and SO_2 emissions are difficult to be achieved simultaneously. In this section, the impact of decision makers on the objectives is taken into account. If the decision makers have preferences in the two objections, the two objectives should be considered at the same time. Thus, this paper combines the proposed method and CPLEX to obtain a set of Pareto solutions for the decision makers. The Pareto solutions are presented in Fig. 5, in which the horizontal and vertical axes represent the total fuel cost and total SO_2 emissions, respectively. The model can provide a solution for the decision maker after obtaining a set of Pareto solutions. It can be seen from Fig. 5 that 50 Pareto solutions can be generated by using the proposed model. From the Pareto frontier solution obtained, it is clear that there is a conflict between the two objectives. In addition, this paper can help the decision makers choose the best solution for each stage.

It can be concluded from the figure that when SO_2 emissions are ignored, the total cost for shipping can be reduced to f_1^I = 256,714.30 USD, and the total SO_2 emissions are f_2^N= 39.285 tons. When the impact of the total fuel cost is ignored, the total SO_2 emissions can be reduced to f_2^I= 23.589 tons, but the total fuel cost increases to f_1^N= 263,056.40 USD. That is to say, using SO_2 emissions as an objective function can reduce the pollutant by 15.696 tons, but the total cost will increase 6,342.10 USD. This also indicates that there are contradictions between the two objectives.

To help the decision makers to obtain their preferred solutions, we assume that there are three types of preferences. In the first scenario, the weight for the first objective is ω_1= 0.8. In the second scenario, the two objectives are treated equally, i.e., ω_1= 0.5. In the last scenario, the decision makers pay more attention to environmental pollution, so ω_1= 0.2. The three solutions are shown in Fig. 5. It can be seen that different weights can lead to different Pareto solutions. The solutions are illustrated in Table 5, in which Δf_1 is the cost growth rate for f_1^I, i.e., $\Delta f_1 = (F_1 - f_1^I)/(f_1^N - f_1^I)$, and Δf_2 is the reduction rate of total SO_2 emissions, i.e., $\Delta f_2 = (f_2^N - F_2)/(f_2^N - f_2^I)$.

It can be seen from Table 5 that the total membership degree of a single optimal solution is high, which is from 0.651 to 0.784. If the decision makers pay more attention to the cost, the selected solution (ω_1=0.8) shows that the cost will only grow 9.69%, while the total SO_2 emissions will be reduced by 25.00%. If the decision makers concern more about the environment issues, the selected solution (ω_1=0.2) shows that the total cost will increase 91.37% with SO_2 emissions

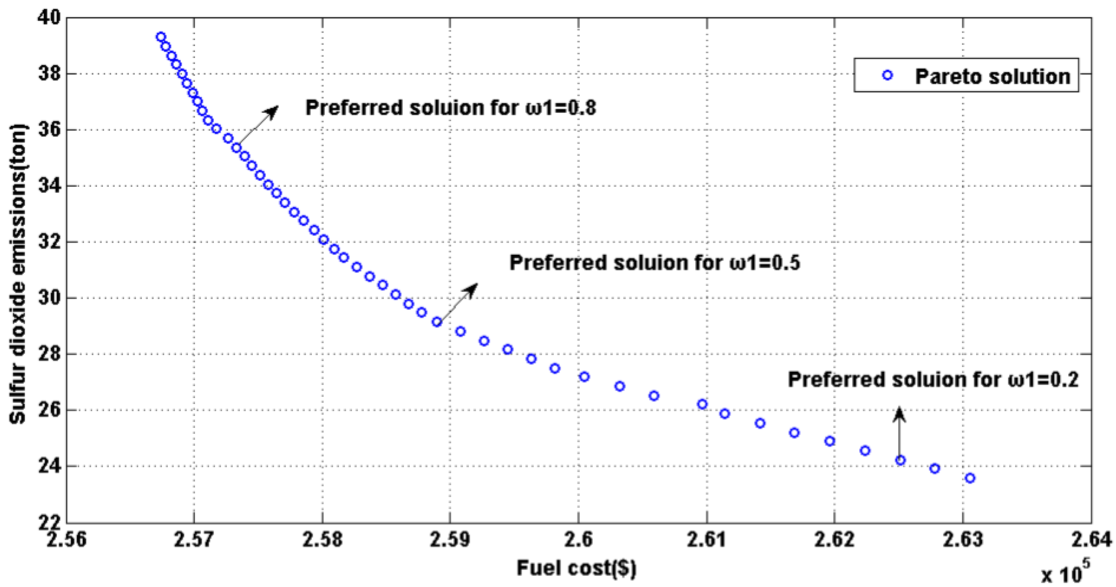

Figure 5: The approximate Pareto frontier of the example

Table 5: Details of the solutions based on different preferences of decision makers

ω_1	δ^s	F_1 (USD)	F_2 (tons)	$\Delta f_1(\%)$	$\Delta f_2(\%)$
0.8	0.772	257329.15	35.361	9.69	25.00
0.5	0.651	258899.15	29.148	34.45	64.58
0.2	0.784	262508.82	24.243	91.37	95.83

reduced by 95.83%.

5.2.4. Effect of ECA boundary

In this section, the impact brought by the ECA policy is analyzed by changing the boundary of ECA. Five situations are considered based on the existing ECA: setting the boundary of ECA 4 nautical miles closer to the coastline (L_1), 2 nautical miles closer to the coastline (L_2), remaining the boundaries of ECA unchanged (L_3), setting the boundary of ECA 2 nautical miles further from the coastline (L_4), 4 nautical miles further from the coastline (L_5). From Table 6, we can see that among all situations, the average sailing speed outside the ECA in situation L_2 is at the maximum value, while the average sailing speed within the ECA in situation L_3 is at the minimum value. The total fuel consumption increases from L_1 to L_5 within the ECA, while decreases outside the ECA. It can also be seen that in the three cases, with the expansion of the ECA, the total cost of fuel increases, while the total SO_2 emissions decrease. The ECA boundary is set up primarily to minimize the total SO_2 emissions and reduce environmental pollution at a reasonable cost. In this example, different boundaries of ECA will have different impacts on shipping industry. The results show that L_3 is a suitable ECA boundary.

Table 6: The total fuel cost and SO_2 emissions under different boundaries of ECA

Five situations		L_1	L_2	L_3	L_4	L_5
Average speed (knots)	Inside ECA	15.212	15.623	15.101	15.802	15.634
	Outside ECA	16.491	16.532	16.206	16.307	16.145
Total fuel consumption (tons)	Inside ECA	113.939	119.144	122.228	135.153	137.535
	Outside ECA	421.502	415.966	412.909	403.618	399.908
Total cost (USD)	$\omega_1 = 0.8$	253963.180	254780.820	257329.150	261738.340	262717.050
	$\omega_1 = 0.5$	256162.560	257824.230	258899.150	264830.040	265113.990
	$\omega_1 = 0.2$	258514.340	260237.020	262508.820	268456.230	269266.860
Total SO_2 emissions (tons)	$\omega_1 = 0.8$	35.946	35.569	35.361	34.737	34.481
	$\omega_1 = 0.5$	29.733	29.356	29.148	28.524	28.269
	$\omega_1 = 0.2$	24.828	24.451	24.243	23.619	23.363

We select 10 routes (denoted by S_1-S_{10}) from regions all over the world: the Baltic Sea area, the North Sea area, the North America area, the United States Caribbean Sea area, the sea areas near China and other sea areas. Specific routes are presented in Fig. 6 and Table 7.

Table 7: Detailed information about the 10 routes

No.	Paths
S_1	1 Tianjin – 2 Shanghai – 3 Wenzhou – 4 Guangzhou
S_2	5 Weihai – 6 Qingdao – 2 Shanghai – 7 Xiamen
S_3	2 Shanghai – 7 Xiamen – 8 Hong Kong – 9 Tokyo
S_4	10 Kodiak – 11 Steattle – 12 Los Angeles – 13 Manzanillo
S_5	14 Vancouver – 15 San Francisico – 12 Los Angeles – 16 Honolulu
S_6	17 New York – 18 Port Canaveral – 19 Miami – 20 Great Strirrup Cay – 21 Nassau
S_7	22 Halifax – 17 New York – 19 Miami – 23 San Juan(Puerto Rico)
S_8	22 Halifax – 17 New York – 24 Wilmington – 25 Ponta delgada
S_9	26 Bibuo – 27 Cherbourg – 28 Dublin – 29 Kristiansand
S_{10}	30 Lisbon – 27 Cherbourg – 31 Glasgow – 32 Hamburg

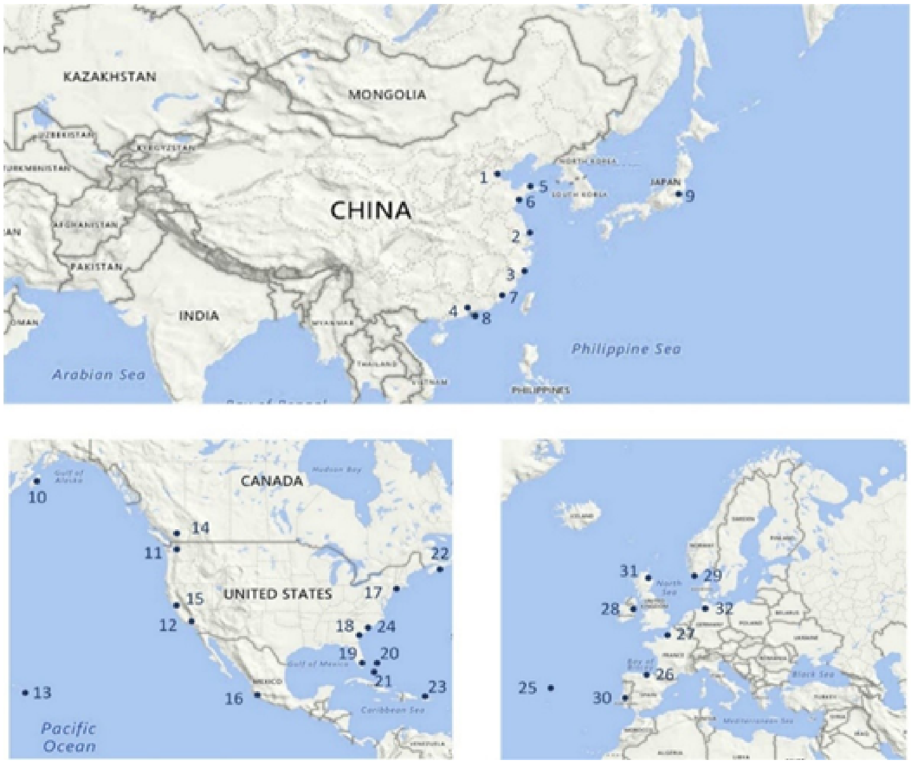

Figure 6: The Distribution of ports around the ten routes

The results are presented in Fig. 7. The dashed lines indicate the total fuel cost and the solid lines represent the total SO_2 emissions. The blue, black, and red lines represent $\omega = 0.8$, $\omega = 0.5$ and $\omega = 0.2$, respectively. The horizontal coordinates represent five scenarios of the ECA boundary, and the longitudinal coordinates represent the total fuel cost and total SO_2 emissions. The results show that there are three situations. First, from case 1 and case 4, the trends of the two objective functions are "V-shaped". In situation L_3, the total fuel cost and SO_2 emissions reach the minimization values, and the optimal solution is L_3. Second, from case 5, case 6, and case 8, it can be concluded that under the three situations, the total fuel cost increases with the expansion of ECA boundaries, while the trend of total SO_2 emissions is "V-shaped", and the minimal solution is obtained near situation L_3. The main goal of ECA is to minimize the total SO_2 emissions at the possible lowest cost, and thus the optimal boundary of ECA should be at L_3. Third, from case 2, case 3, case 7, case 9, and case 10, experimental results show that the total fuel cost increases and the total SO_2 emissions reduce with the expansion of ECA boundary in three different decision-making situations. Therefore, the optimal solution should be near L_3. Based on the average value of the results from the 10 routes, although there may exist situations in which the performance of

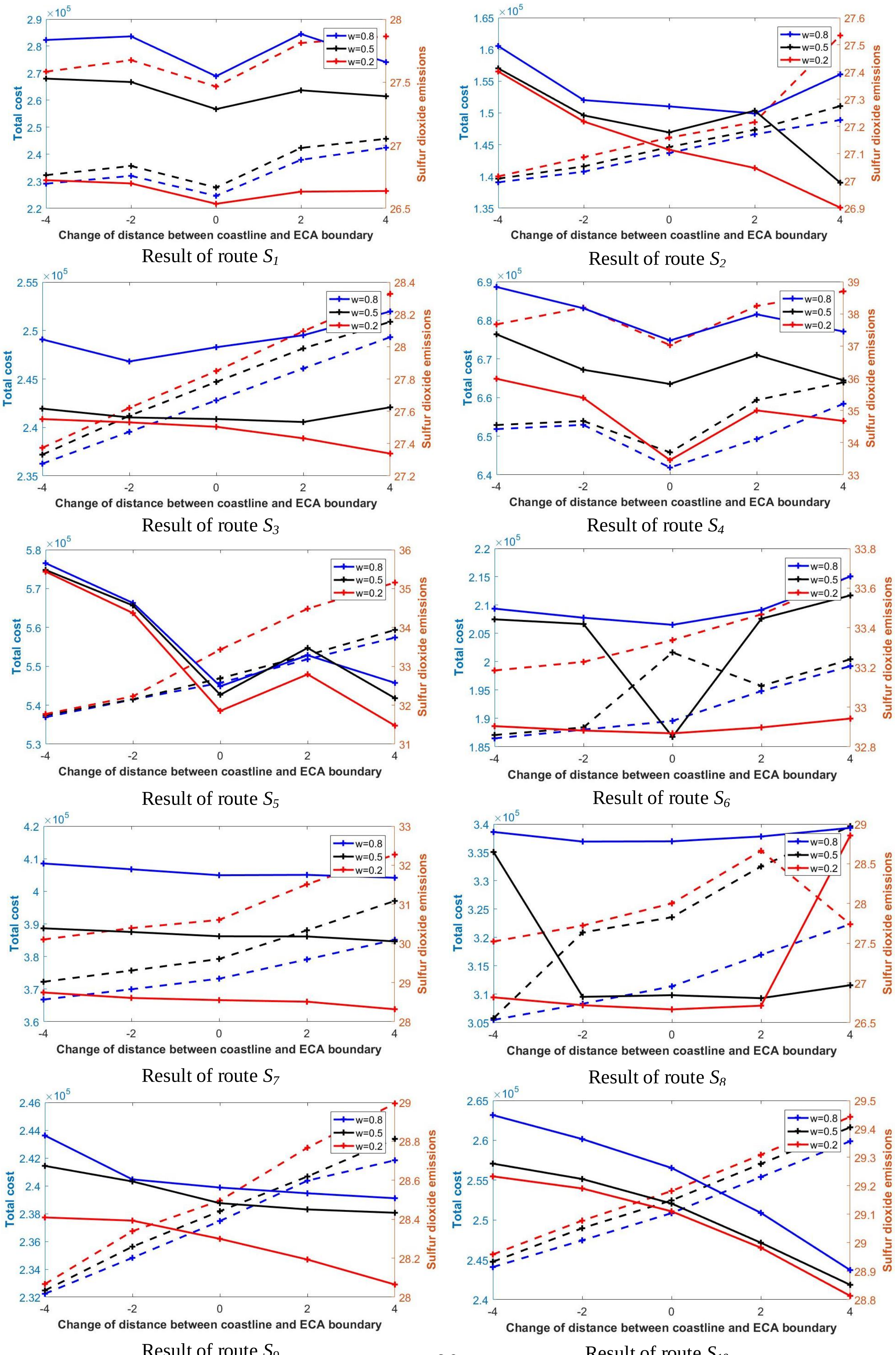

Figure 7: Changes of the total fuel cost and SO_2 emissions with boundaries of the ECA for the 10 routes

the two objective functions is better than that in situation L_3, the overall optimal choice of the ECA boundary should still be L_3.

To sum up, the bi-objective route and speed optimization model proposed in this paper is effective under the restriction of ECA policy. When the membership weights of the two objective functions are the same, the total fuel cost and SO_2 emissions of the container liners within and outside the ECA will be significantly reduced by the proposed model considering the effects of ECA. In real situations, the decision makers can choose suitable solutions according to their preference. The model can also be used to validate the effectiveness of the design of the ECA boundary, save the operating costs of companies, and reduce SO_2 emissions to improve their social image.

6. Conclusions

Under the emission control policy, shipping routes and speeds optimization are important strategic decisions for liner shipping companies. In this paper, a bi-objective mixed integer programming model is constructed, and the voyage plan is reformulated by optimizing the shipping speed and routes. The objectives of this model are to minimize the total fuel cost and SO_2 emissions within and outside the ECA. The model is solved by adopting a two-stage iterative method based on ϵ-constraint. Finally, the actual container liner navigation data of the company is used for the numerical experiments. The effectiveness and practicability of the ECA boundary division are validated by the model, and different solutions are provided for the decision makers. The contributions of this paper are as follows.

(1) This paper proposes a bi-objective model to optimize the shipping routes and speed of the container liners. The results show that when the membership degrees of the two objective functions are the same and the ECA regulations are considered, the container liners are more likely to opt for longer routes to reduce the shipping distance within the ECA. In addition, the shipping speed in the ECA will be reduced while the speed outside the ECA will be increased to satisfy the time window requirements of the ports.

(2) This paper also takes the fluctuation of the fuel price all over the world into consideration and analyzes the cost savings under different fuel prices. It can be seen that the larger difference the fuel price within and outside the ECA, the more savings the model can achieve. The optimization

analysis of the example further validates the effectiveness of the model and can also provide great significance to the development of shipping industry.

(3) In order to solve the proposed bi-objective mixed integer linear programming optimization model, a two-stage iterative method based on ϵ-constraint is designed. Based on the two objective functions, the searching space of the proposed ϵ-constraint method is narrowed, and thus the searching time for the Pareto optimal solutions is reduced. Moreover, this method can provide a set of Pareto optimal solutions for the decision makers to help them choose the optimal solution under the policy of emission control.

(4) Ten shipping routes are included and analyzed by searching the ports within ECAs in China, America, and Europe. By changing the boundaries of the ECAs, the efficiency and practicality of the design of ECA are validated. It is suggested that the shipping companies should use clean energy, low sulfur fuel, filter devices, and on-line monitoring devices, as well as eliminate the old ships to better respond to the increasingly strict sulfur-limiting measures and promote the development of green shipping.

The main goal of establishing the ECAs is to reduce SO_2 emissions (as well as NO_x in North America). According to related research, the reduction of SO_2, NO_x and PM emissions within ECAs is significant and promising. Although there are a large number of sea areas and shipping routes all over the world, the 10 shipping routes in different sea areas are representative. ECA is an important part under the concept of "green shipping". The choices of shipping speeds and routes under the policy of ECA are key and complex issues, which include model construction and solution, and the choice of subjective and objective factors. When stricter rules on sulfur emissions are implemented, this paper can shed light on the redesign of ECA's boundaries. This research can not only present the solution of the optimal shipping speeds and routes for companies and states but also be applied to ECA establishment in other areas. For example, the ECA establishment in the Mediterranean.

Acknowledgments

This work was supported by the National Natural Science Foundation of China [Grant numbers 71831008, 71671107] and the Research Grants Council of the Hong Kong Special Administrative Region, China [Project number 15200817].

References

Acciaro, M., 2014. Real option analysis for environmental compliance: LNG and emission control areas. *Transportation Research Part D: Transport and Environment* 28(2), 41-50.

Bell, M. G. H., Liu, X., Rioult, J., Angeloudis, P., 2013. A cost-based maritime container assignment model. *Transportation Research Part B: Methodological* 58, 58-70.

Bergqvist, R., Turesson, M., Weddmark, A., 2015. Sulphur emission control areas and transport strategies - the case of Sweden and the forest industry. *European Transport Research Review* 7(2), 10-20.

B*é*rub*é*, J. F., Gendreau, M., Potvin, J. Y., 2009. An exact ϵ-constraint method for bi-objective combinatorial optimization problems: application to the traveling salesman problem with profits. *European Journal of Operational Research* 194(1), 39-50.

Boscaratoa, I., Hickeya, N., Ka*š*para, J., Pratib, M. V., Mariani, A., 2015. Green shipping: Marine engine pollution abatement using a combined catalyst/seawater scrubber system.1.Effect of catalyst. *Journal of Catalysis* 328, 248-257.

Browning, L., Hartley, S., Bandemehr, A., Gathright, K., Miller, W., 2012. Demonstration of fuel switching on oceangoing vessels in the gulf of Mexico. *Journal of the Air* & *Waste Management Association* 62(9), 1093-1101.

Chen, L., Yip, T. L., Mou, J., 2018. Provision of Emission Control Area and the impact on shipping route choice and ship emissions. *Transportation Research Part D: Transport and Environment* 58, 280-291.

Cheong, C. Y., Tan, K. C., 2008. A multi-objective multi-colony ant algorithm for solving the berth allocation problem. *Advances of Computational Intelligence in Industrial Systems* 116, 333-350.

Cullinane, K., Bergqvist, R., 2014. Emission control areas and their impact on maritime transport. *Transportation Research Part D: Transport and Environment* 28, 1-5.

Demir, E., Bektas, T., Laporte, G., 2014. The bi-objective pollution-routing problem. *European Journal of Operational Research* 232(3), 464-478.

Doudnikoff, M., Lacoste, R., 2014. Effect of a speed reduction of containerships in response to higher energy costs in sulphur emission control areas. *Transportation Research Part D: Transport and Environment* 28, 51-61.

Dulebenets, M. A., Golias, M. M., Mishra, S., 2015. The green vessel schedule design problem: consideration of emissions constraints. *Energy Systems* 8(4), 1-23.

Dulebenets, M. A., 2017. The green vessel scheduling problem with transit time requirements in a liner shipping route with emission control areas. *Alexandria Engineering Journal* 57(1), 31-37.

Du, Y., Chen, Q., Quan, X., Long, L., Fung, R. Y. K., 2011. Berth allocation considering fuel consumption and vessel emissions. *Transportation Research Part E: Logistics and Transportation Review* 47(6), 1021-1037.

Fagerholt, K., Gausel, N. T., Rakke, J. G., Psaraftis, H. N., 2015. Maritime routing and speed optimization with emission control areas. *Transportation Research Part C: Emerging Technologies* 52, 57-73.

Fagerholt, K., Psaraftis, H. N., 2015. On two speed optimization problems for ships that sail in and out of emission control areas. *Transportation Research Part D: Transport and Environment* 39(1), 56-64.

Gu, Y., Wallace, S. W., 2017. Scrubber: a potentially overestimated compliance method for the emission control areas. *Transportation Research Part D: Transport and Environment* 55, 51-66.

Haimes, Y. Y., Lasdon, L. S., Wismer, D. A., 1971. On a bicriterion formulation of the problems of integrated system identification and system optimization. *IEEE Transactions on Systems, Man & Cybernetics* 1(3), 296-297.

Hilmola, O. P., 2015. Shipping sulphur regulation, freight transportation prices and diesel markets in the Baltic Sea region. *International Journal of Energy Sector Management* 9(1), 120-132.

Jiang, L., Kronbak, J., Christensen, L. P., 2014. The costs and benefits of sulphur reduction measures: sulphur scrubbers versus marine gas oil. *Transportation Research Part D: Transport and Environment* 28(2), 19-27.

Kim, K. H., Moon, K. C., 2003. Berth scheduling by simulated annealing. *Transportation Research Part B: Methodological* 37(6), 541-560.

Kisialiou, Y., Gribkovskaia, I., Laporte, G., 2018. Robust supply vessel routing and scheduling. *Transportation Research Part C: Emerging Technologies* 90, 366-378.

Kisialiou, Y., Gribkovskaia, I., Laporte, G., 2019. Supply vessel routing and scheduling under uncertain demand. *Transportation Research Part C: Emerging Technologies* 104, 305-316.

Kontovas, C. A., 2014. The green ship routing and scheduling problem (GSRSP): a conceptual approach. *Transportation Research Part D: Transport and Environment* 31(5), 61-69.

Lindstad, H., Asbjϕrnslett, B. E., Jullumstrϕ, E., 2013. Assessment of profit, cost and emissions by varying speed as a function of sea conditions and freight market. *Transportation Research Part D: Transport and Environment* 19(5), 5-12.

Li, Y., Chu, F., Chu, C., Zhou, W., Z., 2016. Integrated production inventory routing planning with time windows for perishable food. *IEEE Transactions on Intelligent Transportation Systems*, 2651-2656.

Mavrotas, G., 2009. Effective implementation of the ϵ-constraint method in Multi-Objective Mathematical Programming problems. *Applied Mathematics* & *Computation* 213(2), 455-465.

Meisel, F., Bierwirth, C., 2009. Heuristics for the integration of crane productivity in the berth allocation problem. *Transportation Research Part E: Logistics and Transportation Review* 45(1), 1-23.

Meng, Q., Wang, S., 2012. Liner ship fleet deployment with week-dependent container shipment demand. *European Journal of Operational Research* 222(2), 241-252.

Meng, Q., Wang, S., Andersson, H., Thun, K., 2014. Containership routing and scheduling in liner shipping: overview and future research directions. *Transportation Science* 48(2), 265-280.

Moorthy, R., Teo, C. P., 2006. Berth management in container terminal: the template design problem. *OR Spectrum* 28(4), 495-518.

Msakni, M. K., Haouari, M., 2018. Short-term planning of liquefied natural gas deliveries. *Transportation Research Part C: Emerging Technologies* 90, 393-410.

Ng, M. W., 2014. Distribution-free vessel deployment for liner shipping. *European Journal of Operational Research* 238(3), 858-862.

Ng, M. W., 2015. Container vessel fleet deployment for liner shipping with stochastic dependencies in shipping demand. *Transportation Research Part B: Methodological* 74, 79-87.

Ng, M. W., 2018. Vessel speed optimisation in container shipping: A new look. *Journal of the Operational Research Society* 70(4), 541-547.

Norstad, I., Fagerholt, K., Laporte, G., 2011. Tramp ship routing and scheduling with speed optimization. *Transportation Research Part C: Emerging Technologies* 19(5), 853-865.

Panasiuk, I., Turkina, L., 2015. The evaluation of investments efficiency of SO_x scrubber installation. *Transportation Research Part D: Transport and Environment* 40, 87-96.

Park, Y. M., 2003. A scheduling method for berth and quay cranes. *OR Spectrum* 25(1), 1-23.

Patricksson, ϕ. S., Fagerholt, K., Rakke, J. G., 2015. The fleet renewal problem with regional emission limitations: case study from roll-on/roll-off shipping. *Transportation Research Part C: Emerging Technologies* 56, 346-358.

Psaraftis, H. N., Kontovas, C. A., 2013. Speed models for energy-efficient maritime transportation: a taxonomy and survey. *Transportation Research Part C: Emerging Technologies* 26(26), 331-351.

Psaraftis, H. N., Kontovas, C. A., 2014. Ship speed optimization: concepts, models and combined speed-routing scenarios. *Transportation Research Part C: Emerging Technologies* 44, 52-69.

Psaraftis, H. N., 2019. Speed Optimization for sustainable shipping. In: Harilaos N. Psaraftis (Ed.), Sustainable Shipping. Springer, Cham, pp. 339-374.

Schinas, O., Stefanakos, C. N., 2012. Cost assessment of environmental regulation and options for marine operators. *Transportation Research Part C: Emerging Technologies* 25(8), 81-99.

Sheng, D., Meng, Q., Li, Z. C., 2019. Optimal vessel speed and fleet size for industrial shipping services under the emission control area regulation. *Transportation Research Part C: Emerging Technologies* 105, 37-53.

Song, D. P., Dong, J. X., 2012. Cargo routing and empty container repositioning in multiple shipping service routes. *Transportation Research Part B: Methodological* 46(10), 1556-1575.

Song, D. P., Dong, J. X., 2013. Long-haul liner service route design with ship deployment and empty container repositioning. *Transportation Research Part B: Methodological* 55, 188-211.

Song, D. P., Li, D., Drake, P., 2015. Multi-objective optimization for planning liner shipping service with uncertain port times. *Transportation Research Part E: Logistics and Transportation Review* 84, 1-22.

Svindland, M., 2018. The environmental effects of emission control area regulations on short sea shipping in Northern Europe: The case of container feeder vessels. *Transportation Research Part D: Transport and Environment* 61, 423-430.

Tian, G., Zhou, M. C., Li, P., Zhang, C., Jia, H., 2016a. Multiobjective optimization models for locating vehicle inspection stations subject to stochastic demand, varying velocity and regional constraints. *IEEE Transactions on Intelligent Transportation Systems* 17(7), 1978-1987.

Tian, G., Ren, Y., Zhou, M. C., 2016b. Dual-Objective scheduling of rescue vehicles to distinguish forest fires via differential evolution and particle swarm optimization combined algorithm. *IEEE*

Transactions on Intelligent Transportation Systems 17(11), 3009-3021.

Wang, S., Meng, Q., 2012. Sailing speed optimization for container ships in a liner shipping network. *Transportation Research Part E: Logistics and Transportation Review* 48(3), 701-714.

Wang, S., Meng, Q., 2017. Container liner fleet deployment: a systematic overview. *Transportation Research Part C: Emerging Technologies* 77, 389-404.

Wang, Y., Meng, Q., Du, Y., 2015. Liner container seasonal shipping revenue management. *Transportation Research Part B: Methodological* 82, 141-161.

Wang, Y., Meng, Q., Kuang, H., 2018. Jointly optimizing ship sailing speed and bunker purchase in liner shipping with distribution-free stochastic bunker prices. *Transportation Research Part C: Emerging Technologies* 89, 35-52.

Yeung, S., Man, K., 2011. Multiobjective optimization. *IEEE Microwave Magazine* 12(6), 120-133.

Zhen, L., Li, M., Hu, Z., Lv, W., Zhao, X., 2018. The effects of emission control area regulations on cruise shipping. *Transportation Research Part D: Transport and Environment* 62, 47-63.